SINGULAR-FPZ MODEL FOR NUMERICAL SIMULATION OF DYNAMIC FRACTURE OF CONCRETE

Jung-Heum Yon [1], Neil M. Hawkins [1] and Albert S. Kobayashi [2]

Nonsingular- and singular-FPZ models were used to replicate numerically, dynamic fracture of displacement-controlled and drop-weight three-point bend specimens and a CLWL-DCB specimen. This numerical analysis showed that the singular-FPZ model provided the most realistic simulation of dynamic fracture of concrete. The resulting constitutive relation between the crack closure stress and crack opening displacement for the singular-FPZ model was geometry and strain rate independent. The stress intensity factor, however, was strain rate dependent.

INTRODUCTION

A dynamic fracture model based on linear elastic fracture mechanics (LEFM) does not adequately represent the fracture response of concrete since this model does not account for the crack closure stress (CCS) generated by aggregate bridging and interlock which trails a propagating crack tip in concrete [1]. This deficiency was eliminated by a new finite element method of continuous crack propagation in concrete using a singular-FPZ model which is presented in this paper. That new numerical technique and constitutive model for the fracture process zone (FPZ) was used to reanalyze the results of dynamically loaded, displacement-controlled and drop-weight bend specimens [2,3] as well as to analyze the dynamic fracture data of a crack-line wedge-loaded double-cantilever beam (CLWL-DCB) specimen [4]. The results obtained with that singular-FPZ model are also compared with those predicted using an FPZ model or a nonsingular-FPZ model developed previously [2].

[1] Department of Civil Engineering, University of Washington, Seattle, WA 98195.
[2] Department of Mechanical Engineering, University of Washington, Seattle, WA 98195.

SINGULAR-FPZ MODEL

The singular-FPZ model proposed here is similar to the two parameter model [5,6] involving a critical stress intensity factor, K_{IC}, at an effective crack tip and a critical crack tip opening displacement, $CTOD_C$, both of which are used as the fracture criteria. The singular-FPZ model of this paper uses as a fracture criterion only the dynamic stress intensity factor, K_{ID}, at the micro-crack tip which is trailed by an FPZ. The effect of the FPZ is to reduce the stress intensity factor through a CCS generated by aggregate bridging. Thus the CCS in the FPZ decrease with increasing crack opening displacement (COD) where the CCS is assumed to be uniquely related to the COD.

HYBRID EXPERIMENTAL-NUMERICAL ANALYSIS

The mechanical properties of concrete under dynamic load were determined by using a hybrid experimental-numerical technique in its application mode [4]. In this study, the load history together with an assumed CCS and COD relation were used as input boundary conditions for the two-dimensional dynamic finite element analysis. The numerical results, which was generated by this inverse process, were then compared with those measured experimentally. The procedure was repeated until the assumed dynamic elastic and fracture properties yielded numerical results consistent with the experimental results.

RESULTS

Figure 1 shows the geometry and strain gage locations for the three-point bend specimen with a precast single-edge notch used for the displacement-controlled and drop-weight bend tests. Figure 2 shows the geometry and strain gage locations for the CLWL-DCB specimen. A 12.7 *mm* saw-cut notch was made at the precast notch tip of that specimen in an attempt to remove the damage caused by drying shrinkage at the precast notch tip. SG01, SG02 and SG03 represent three strain gages which provided detailed strain histories during the fracture process.

Two non-contact capacitance gages were used to measure load-line displacements for the displacement-controlled bend test and the crack-line displacements, $2V_1$ and $2V_2$, for the displacement-controlled CLWL-DCB test. The load-line displacement, $2V_p$, from the CLWL-DCB test was determined by linear interpolation of the $2V_1$ and $2V_2$ results. In the drop-weight test, the load-line displacement was not recorded but the COD variations of a propagating crack were determined from transient Moiré interferometry fringes.

Table 1: Measured and Optimized Mechanical Properties

	Displacement-Controlled Bend Test	Drop-Weight Bend Test	CLWL-DCB Test
Concrete Mix (by weight)	Cement : Gravel : Sand : Water = 1.0 : 2.0 : 2.5 : 0.4 – 0.5		
Static Compression Strength (MPa)	49.1	55.1	56.0
Static Splitting Strength (MPa)	–	3.96	4.04
Dynamic Stress Intensity Factor ($MNm^{-1.5}$)	1.90	1.98	1.88
Dynamic Elastic Modulus (GPa)			
Tension	55.2	34.5	58.6
Compression	62.1	41.4	58.6
Crack Tip Element	12.4	12.4	58.6
Fracture Energy Density (N/m)			
Nonsingular-FPZ Model	156	184	161
Singular-FPZ Model	158	157	157

The dynamic mechanical properties was optimized when the FEM model yielded computed strains which matched the three measured strains at SG01, SG02 and SG03 or the computed COD's matched those measured by Moiré interferometry. The measured and optimized mechanical properties obtained by this hybrid experimental-numerical technique are shown in Table 1. The elastic modulus at the initial crack tip was purposefully reduced to simulate damage caused by drying shrinkage. The resultant CCS and COD relations are shown in Figure 3. Nonsingular-FPZ results are indicated by the squares and singular-FPZ results by the circles. For the singular-FPZ model, the relations are essentially geometry and strain rate independent.

Figures 4, 5 and 6 show the measured and computed strain histories for each test using the nonsingular- and singular-FPZ models. The singular-FPZ model simulated more accurately the strain histories of the first and second gages, SG01 and SG02, respectively. The nonsingular-FPZ model more accurately predicted the strain histories of the third strain gage, SG03. The discrepancy in the third strain, SG03, in Figure 6 is probably due to the crack curving away from the center line of the specimen after 120 mm of crack extension. A straight crack propagation had been assumed for the numerical analysis.

The main difference obtained by the nonsingular- and singular-FPZ models is the COD variations with crack propagation as shown in Figure 7 for the drop-weight bend test. The COD variations measured by the Moiré in-

terferometry fringes were parabolic in shape at the crack tip and agreed with the predictions of the singular-FPZ model but not with the nonsingular-FPZ model. The computed COD variations for the displacement-controlled bend test and the CLWL-DCB test showed the same trends.

DISCUSSIONS

The crack extension histories show that the crack velocity for the drop-weight bend test was only 80 percent faster than that for the displacement-controlled bend test, even though the strain rate increased about three times.

Figure 8 shows the computed energy partitions of each test. The maximum strain energy in the drop-weight bend test was 2.4 times of that in the displacement-controlled bend test. However, Table 1 shows that the average elastic modulus for the drop-weight bend test was 45 percent less than that of the displacement-controlled bend test. The lower elastic modulus of the drop-weight test, despite the faster strain rate of loading, can be attributed to the added damage caused by the drying shrinkage. Table 1 also shows that the dynamic stress intensity factor may be geometry independent but strain rate dependent.

Figure 9 shows the energy release rate and dissipation rate at the FPZ in the specimen. The remarkable coincidence between the two rates indicates that the dominant energy dissipation mechanism in concrete is at the FPZ. Dynamic fracture resistance of concrete can thus be increased if the dissipation energy rate in the fully developed FPZ can be increased. Larger aggregate size, concrete composite with embedded fibers all contribute to such increase in the dissipated energy in the FPZ.

CONCLUSIONS

A finite element model of a rapidly fracturing concrete specimen with a singular-FPZ model was developed. This model successfully predicted the fracture responses of displacement-controlled and drop-weight three-point bend tests and CLWL-DCB test. The findings from this study are:

1. The COD variations associated with the singular-FPZ model simulated closely the form of COD's determined from the Moiré interferometry records.

2. The CCS and COD relation for the singular-FPZ model was essentially geometry and strain rate independent, while the dynamic stress intensity factor was strain rate dependent.

3. The dominant energy dissipation mechanism is the FPZ in a fracturing concrete specimen.

ACKNOWLEDGEMENT

The studies reported in this paper were funded by the U.S. Air Force Office of Scientific Research under Grant AFOSR 86-0204. The authors wish to express their appreciation to Dr. Spencer Wu for his continuing support and encouragement.

REFERENCES

[1] Hillerborg, A., Modeér, M. and Petersson, P.-E., "Analysis of Crack Formation and Crack Growth in Concrete by Means of Fracture Mechanics and Finite Elements," in *Cement and Concrete Research*, Vol.6, 1976, pp.773–782.

[2] Yon, J.-H., Hawkins, N.M. and Kobayasi, A.S., "Strain Rate Sensitivity of Concrete Mechanical Properties," *Material Journal*, ACI, accepted in January, 1990.

[3] Du, J.J. Yon, J.-H., Hawkins, N.M., Arakawa, K. and Kobayashi, A.S., "Fracture Process Zone for Concrete for Dynamic Loading," *Material Journal*, ACI, accepted in February, 1990.

[4] Yon, J.-H., "Dynamic Fracture of Concrete," Ph.D. Dissertation, Department of Civil Engineering, University of Washington, Seattle, WA, 1990.

[5] Jenq, Y.-S. and Shah, S.P., "Two Parameter Fracture Model for Concrete," *Journal of Engineering Mechanics*, ASCE, Vol.110, 1985, pp.1227–1241.

[6] John, R. and Shah, S.P., "Mixed Mode Fracture of Concrete Subjected to Impact Loading," *Journal of Structural Engineering*, ASCE, Vol.116, 1990, pp585.–602.

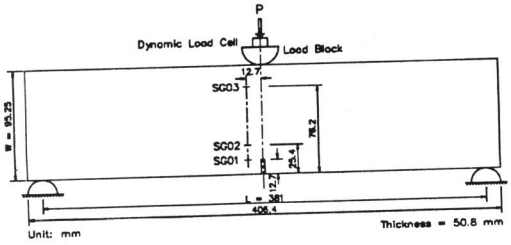

Figure 1: Geometry and Strain Gage Locations of Bend Specimen

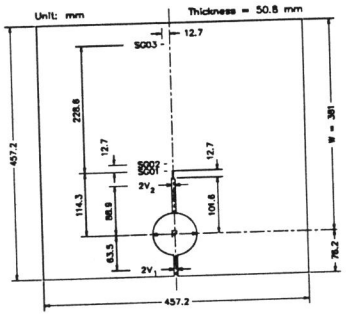

Figure 2: Geometry and Strain Gage Locations of CLWL-DCB Specimen

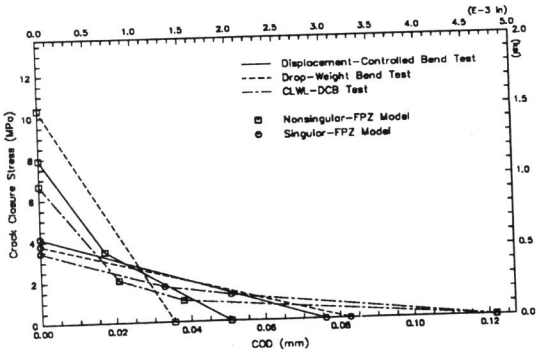

Figure 3: Optimized CCS and COD Relations

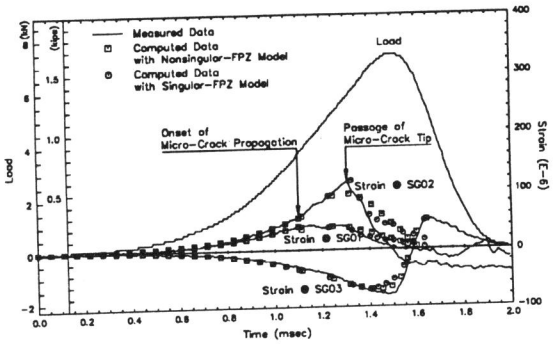

Figure 4: Measured and Computed Strain Histories of Displacement-Controlled Bend Test

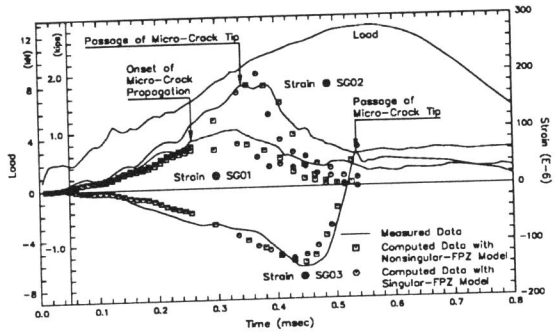

Figure 5: Measured and Computed Strain Histories of Drop-Weight Bend Test

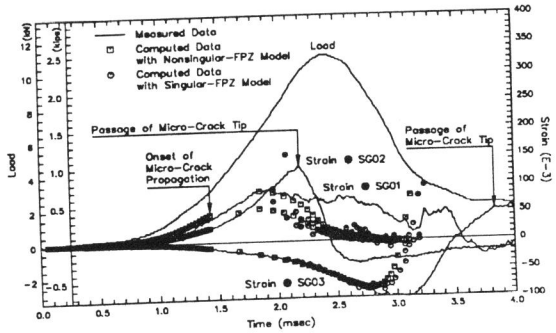

Figure 6: Measured and Computed Strain Histories of CLWL-DCB Test

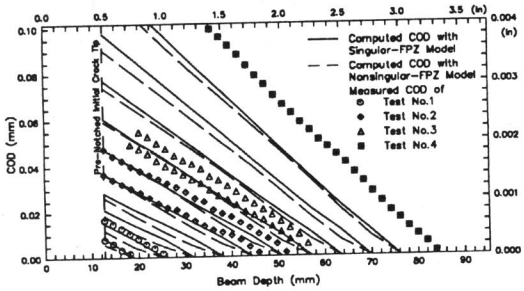

Figure 7: Measured and Computed COD Variations of a Propagating Crack

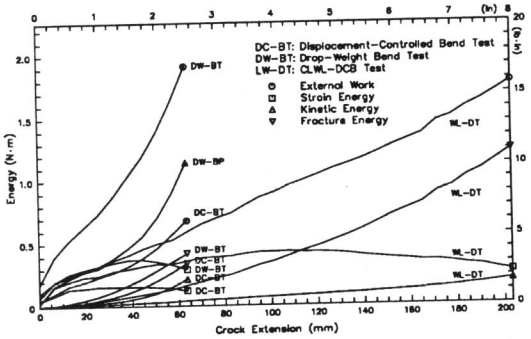

Figure 8: Computed Energy Partitions with Singular-FPZ Model

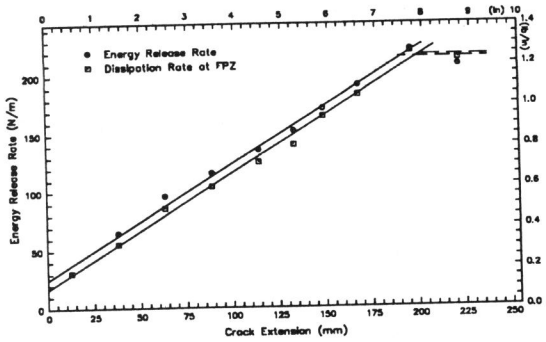

Figure 9: Energy Release Rate and Dissipation Rate at FPZ of CLWL-DCB Specimen